

Effect of Photodoping on the Fiske Resonances of $\text{YBa}_2\text{Cu}_3\text{O}_x$ Grain Boundary Josephson Junctions

M. G. Medici,¹ J. Elly,¹ M. Razani,¹ A. Gilabert,¹ F. Schmidl,² P. Seidel,² A. Hoffmann,³ and Ivan K. Schuller³

Received 3 October 1997

We have expanded our studies on illuminated $\text{YBa}_2\text{Cu}_3\text{O}_x$ grain boundary Josephson junctions (GBJJ) which show both dc Josephson properties (Fraunhofer pattern) and ac Josephson properties (Fiske resonance). Illuminating GBJJs with visible light changes the Josephson coupling. This change is characterized by an increase of the critical current and a large shift in the voltage position of the Fiske resonances. This effect is due to persistent photoinduced superconductivity (PPS) of the oxygen-depleted $\text{YBa}_2\text{Cu}_3\text{O}_x$ barrier, similar to the PPS found in illuminated oxygen-deficient $\text{YBa}_2\text{Cu}_3\text{O}_x$ thin films. From Fiske resonance experiments in GBJJs of different lengths, it is possible to study the velocity of the electromagnetic wave in the barrier and its change after illumination. Information on the parameters of the barrier, before and after illumination, is obtained from this study.

KEY WORDS: High- T_c superconductors; photoconductivity; Josephson effects.

1. INTRODUCTION

Grain boundary junctions made with high critical temperature superconductors act as Josephson weak links resulting from the low critical current density of the grain boundary (GB). The weak transport properties of the GB is due to the fact that the barrier is an oxygen-deficient $\text{YBa}_2\text{Cu}_3\text{O}_x$ region. In recent papers [1] we have estimated an average concentration of the oxygen content x in the barrier and found $x \approx 6.6$. However, the oxygen concentration has a sharp spatial variation in the barrier on a distance comparable to the coherence length ξ_{ab} which is of atomic scale. Thus the weak link is a rather complicated structure and the junction can be modeled as a superconductor–semiconductor–superconductor (S–Sm–S) junction or even a more complex structure like S–N–Sm–N–S junction where N is a normal

metal. Information on the parameters of the barrier for different GBJJs can be obtained from the study of the electromagnetic waves propagating in the barrier which results from the Fiske resonances. The aim of this paper is to expand earlier studies of the electromagnetic wave velocity propagating in Josephson weak links for GBJJs of different lengths and their change with illumination. Illumination by visible light increases the dc Josephson current, thus changing the Josephson coupling. This change of the weak coupling is due to persistent photoinduced superconductivity (PPS) in the reduced oxygen GB barrier. This PPS is similar to the PPS effect observed in $\text{REBa}_2\text{Cu}_3\text{O}_x$ thin films characterized by an unexpected decrease in the normal-state resistance called persistent photoconductivity [2] (PPC) and an increase of the superconducting properties (critical temperature T_c) upon illumination with the visible light [3–7]. These effects increase with a decreasing oxygen content, persist for long times even when the light is switched off if the junction is kept at low temperature ($T < 100$ K), and relax at room temperature [2,6,7].

A theoretical model which explains qualitatively the photoinduced effect is based on the trapping of

¹L.P.M.C. UMR 6622 CNRS, Université de Nice Sophia Antipolis, Parc Valrose 06108, Nice Cedex 02, France.

²Institut für Festkörperphysik, Friedrich-Schiller-Universität Jena, Helmholtzweg 5, D-07743 Jena, Germany.

³Physics Department, University of California-San Diego, La Jolla, CA 92093-0319, USA.

electrons at oxygen vacancies in the CuO chain [8]. In this scenario, an incoming photon produces an electron-hole pair. Subsequently, the electron is trapped at an oxygen vacancy in the CuO chain. The trapped electron causes a lattice distortion, which gives rise to a large energy barrier for the reverse recombination with the hole. The hole is transferred to the CuO₂ plane layer which increases the number of carriers and enhances the conductivity or the superconducting properties.

2. EXPERIMENTS

Details of the fabrication of the GBJJs can be found elsewhere [9]. A YBa₂Cu₃O_x thin film is deposited using an excimer laser ablation process on a bicrystal substrate formed from the fusion of two SrTiO₃ single crystals with misaligned crystal axes. The tilt angles of the bicrystals is around 37°. A Josephson weak link is formed by a grain boundary in the YBa₂Cu₃O_x film grown over the substrate grain boundary. The critical temperatures and the normal state resistance R_N of the GBJJs used are always respectively $T_c \approx 85$ K and a few ohms. The film thickness is $\approx 0.2 \mu\text{m}$ and the length W of the GBJJs studied on the same bicrystal ranges between 4–12 μm . The current-voltage characteristics were measured automatically and registered on a computer at 12 K before and after illumination and for different small applied magnetic field using a closed circuit helium cryostat. The $I(V, H)$ characteristics and therefore the critical currents and the Fraunhofer patterns were unaffected by several temperature cycles and stable over a very long time (several months). The magnetic field is created by a solenoid around the sample. No trapped magnetic flux was observed for magnetic fields below a few gauss and the experimental curves were perfectly reproducible. After one night of relaxation at room temperature in the darkness, the illuminated GBJJs recover the same properties they had before illumination. Illuminating again the GBJJs at low temperature gives reproducible effects. The light used for illumination is provided by a 70 W Hg-Xe lamp which illuminates the whole sample through a window of the optical cryostat.

3. RESULTS AND DISCUSSION

Figure 1 shows current-voltage $I(V)$ characteristics at $T=12$ K for different applied magnetic field in a three-dimensional representation. In the $V=0$ plane the Fraunhofer pattern $I_c(H)$ (also shown in

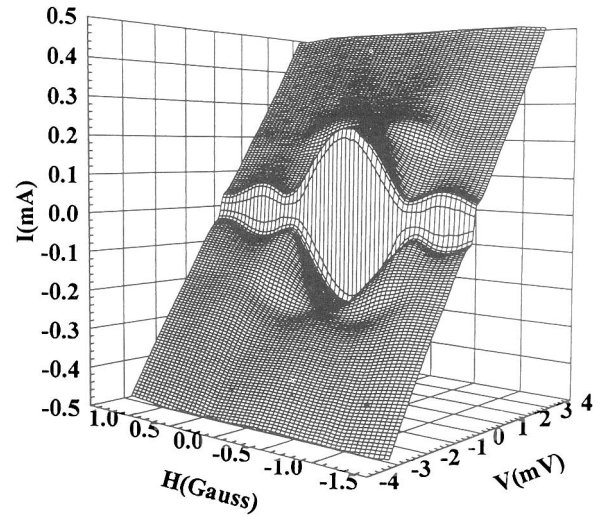


Fig. 1. Current-voltage characteristics of a YBa₂Cu₃O_x GBJJ for different applied magnetic fields.

Fig. 2a) is displayed in good agreement with the theoretical curve $|\sin(\pi\phi)/\pi\phi|$. Here the normalized flux $\phi = \Phi/\Phi_0$, in units of flux quantum $\Phi_0 = h/2e$ (or normalized magnetic fields H/H_0), is flowing perpendicularly through the junction barrier. Figure 1 shows, in addition to the critical current I_c at zero voltage, also the Fiske resonances, which appear as magnetic field-dependent “bumps” at finite voltage [10–12]. Due to high damping in these GBJJs, the structures appear as bumps and not as sharp Fiske steps as usually found in Josephson junctions made with classical superconductor [13]. Four such bumps, whose amplitude is field dependent, are clearly observed in Fig. 1 at a voltage determined by the length W of the GBJJ.

A Josephson junction can be considered as a transmission line for electromagnetic waves. The electric field is essentially confined within the barrier region of thickness t . The magnetic field however, penetrates a larger region of thickness $d = 2\lambda_L + t$, where λ_L is the London penetration depth in the superconducting region. The phase velocity, called the Swihart velocity [13] of an electromagnetic wave for such transmission line, is given by $c = c_0\sqrt{t/\epsilon d}$, where c_0 is the light velocity in vacuum and ϵ the relative dielectric constant of the barrier. In an external magnetic field H , there may be a set of current singularities called Fiske resonances [13] in the $I(V)$ characteristics at voltages

$$V_n = n \left(\frac{h}{2e} \right) \frac{c}{2W} = n\Phi_0 \frac{c}{2W} \quad (1)$$

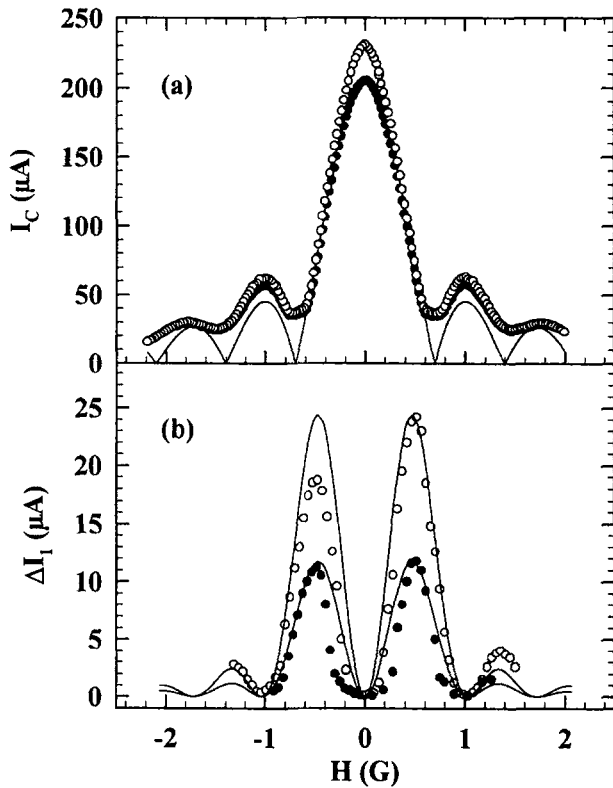


Fig. 2. (a) Critical current vs. magnetic field (Fraunhofer pattern) before (●) and after illumination (○) and theoretical curve $\sin(\pi H/H_0)/(\pi H/H_0)$. (b) Amplitude of the Fiske resonance (first mode) vs. magnetic field before (●) and after illumination (○). The solid line is the theoretical curve F_1^2 given by Eq. (3).

These geometrical resonances occur when the length W of the junction corresponds to a number n of half wavelength of the Josephson current density wave $j=j_c \sin(\omega t - ky)$ running in the y direction along the junction length.

The amplitude $\Delta I(\phi)$ of these resonances as a function of the normalized magnetic flux ϕ through the junction is given theoretically by [13]

$$\Delta I(\phi) = I_c Q \left(\frac{W}{2\pi\lambda_J} \right)^2 F_1^2 \quad (2)$$

with

$$F_1^2 = \left[\frac{2\phi}{\phi + 1/2} \right]^2 \left[\frac{\sin(\pi\phi - \pi/2)}{\pi\phi - \pi/2} \right] \quad (3)$$

where $\lambda_J = \sqrt{\Phi_0/(2\pi\mu_0 d J_c)}$ is the Josephson penetration length, J_c the critical current density, and Q the quality factor. This theoretical function F_1^2 is plotted in Fig. 2b for a typical GBJJ. The experimental results are in a qualitative agreement with this F_1^2 curve as

shown earlier [14]. Comparing the magnetic field periodicity of the Fiske step with the magnetic field periodicity of the Fraunhofer pattern shown in Fig. 2a, we find that the maxima and minima found experimentally are in agreement with the theoretical values [13]: the first maximum of the amplitude of the Fiske step is at $0.7\Phi_0$, the second maximum is at $1.5\Phi_0$, and the first minimum is at Φ_0 .

The effect of 30 min illumination is shown in Figs. 3a and 3b on the $I(V)$ curves at $T=12$ K for $H=0$ G and $H=0.56$ G corresponding to the maximum amplitude of the Fiske bump for the GBJJ used. These curves have been recorded when the light is switched off, so that there is no correction due to heating. The enhancement (11%) of the critical current I_c (Figs. 2a and 3a), the decrease (a few %) of R_N , the increase of the amplitude of the Fiske resonances, and its shift of the voltage positions have been reported earlier for *one* junction [1,14]. For example, in the plane $H=0.56$ G, the position of the Fiske resonance shifts from 0.8 mV for cumulative illumination time until a maximum position $V_1 = 1.15$ mV (see

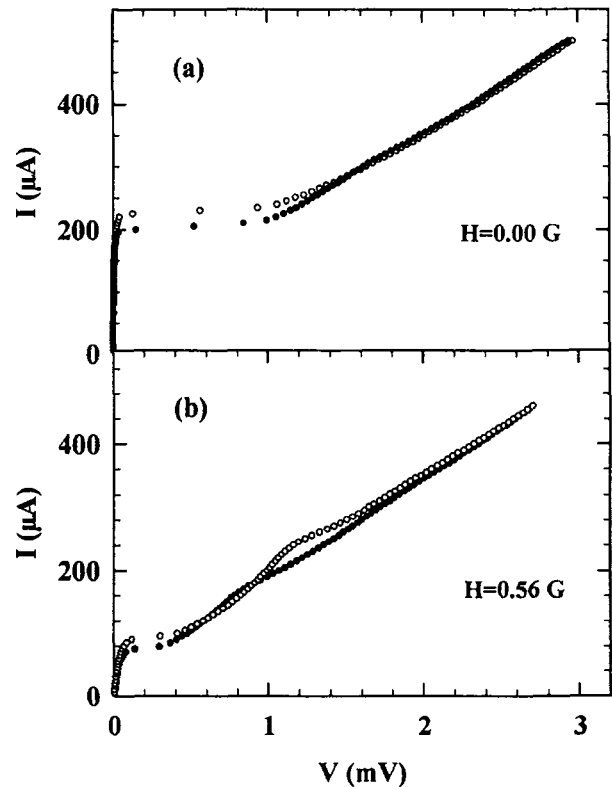


Fig. 3. (a) $I(V)$ curve at $T=12$ K for $H=0$ G before (●) and after illumination (○). (b) $I(V)$ curve at $T=12$ K for $H=0.56$ G corresponding to the maximum amplitude of the Fiske bump before (●) and after illumination (○).

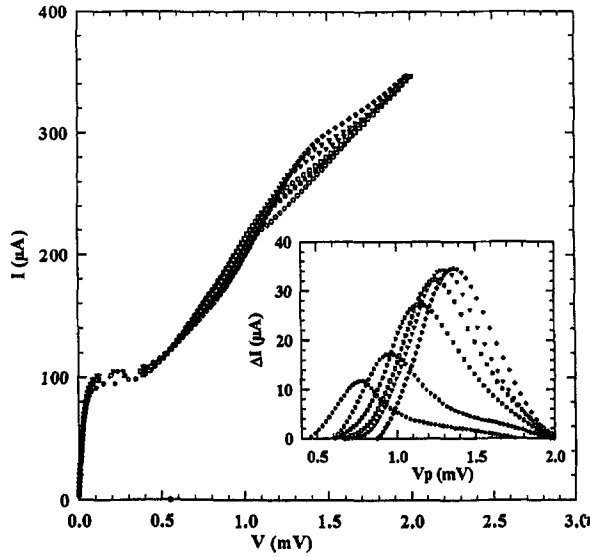


Fig. 4. $I(V)$ curves at $T=12$ K, $H=0.56$ G before illumination and after 0.5, 3, 5, 7, 11, and 20 min illumination time (at low optical power).

Fig. 4) which is a 44% change. In the inset of Fig. 4, the amplitude and position of the Fiske step (obtained by subtracting the background in the $I(V)$ curves) increases gradually until they saturate (0.5–20 min). Here also, the $I(V)$ curves have been recorded in the dark just after different cumulative illumination times. These times are very long because of the very small optical power used.

Figure 2b shows the magnetic field dependence of the maximum amplitude of the Fiske resonance before and after illumination. These dependences vs. H are similar. The Fiske resonance amplitude increases with illumination; however, the minima in the field remain almost unchanged (only a small imbalance is found). This implies that the order n of the Fiske step is unchanged, which allows study of the voltage position of the Fiske resonance vs. the mode number n . Unfortunately the higher-order Fiske resonances are difficult to observe in the original $I(V)$ characteristics. However, subtracting the $I(V)$ curves before and after illumination, as shown in Fig. 5, permits a clear observation of the first three modes. Figure 6 shows the dependence of the voltage positions V_n as a function of n before and after illumination. From this linear slope, and using Eq. (1), we find for the value of the Swihart velocity $c=3.9 \times 10^6$ m/s before illumination and $c=5.5 \times 10^6$ m/s after illumination.

We have studied the maximum voltage position V_1 corresponding to the first Fiske resonances for

GBJJ of different lengths W before and after illumination. Figure 7 shows the linear variation of these voltage positions V_1 as a function of $1/W$ as expected from Eq. (1). The linear slope implies a Swihart velocity $c=4 \times 10^6$ m/s. This linear dependence implies also that GBJJ made on the same bicrystal have homogeneous barriers with the same relative dielectric constant and the same thickness t . These maximum voltage positions V_1 show also a linear variation vs. $1/W$ after illumination (Fig. 7). From the slope we can deduce a value $c=5.6 \times 10^6$ m/s for the Swihart velocity. These values obtained for c before and after illumination are consistent with those found from the voltage position vs. n .

After illumination (noted with the index L), the current $n=1$ bump is at a position $V_L = \Phi_0(c_L/2W)$, where $c_L = c_0 \sqrt{(t_L/\epsilon_L d)}$ is the Swihart velocity after illumination corresponding to an effective dielectric constant ϵ_L . The thickness t_L of the weak link does not change after illumination, because an increase of the Swihart velocity would increase t_L and an increase of the thickness barrier in turn would increase the normal-state resistance and decrease the critical current, the opposite of experimental findings. From the experimental values of the maximum position of the Fiske resonance before and after illumination we deduce if the barrier thickness is constant:

$$\frac{V_L}{V} = \sqrt{\frac{\epsilon}{\epsilon_L}} = 1.44 \quad (4)$$

which gives $\epsilon_L/\epsilon \approx 0.48$.

The photodoping has the effect of decreasing the relative dielectric constant by a factor of ≈ 2 . This effect is related to photodoping of the oxygen-deficient barrier, but the mechanism of the decrease of the dielectric constant is not well understood.

4. CONCLUSION

We have studied the enhancement of the Josephson coupling of GBJJs due to illumination and particularly the shift of the voltage positions of the Fiske resonances after illumination. From the study of the voltage position of the Fiske resonance vs. the inverse of the junction length W or vs. the different modes, it is possible to determine the velocity of the electromagnetic wave in the barrier before and after illumination. The effect of illumination on the low oxygenated $\text{YBa}_2\text{Cu}_3\text{O}_x$ barrier can be understood as due to a decrease of the dielectric constant by photodoping.

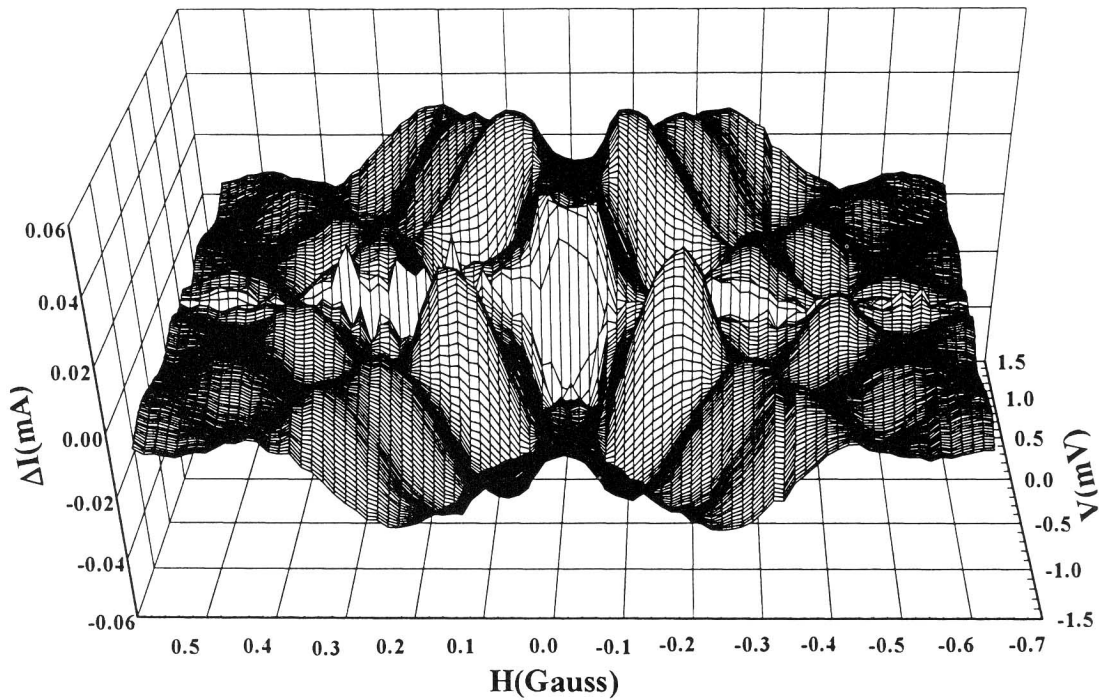


Fig. 5. Difference between the $I(V)$ curves before and the $I(V)$ curves after illumination for different applied magnetic fields.

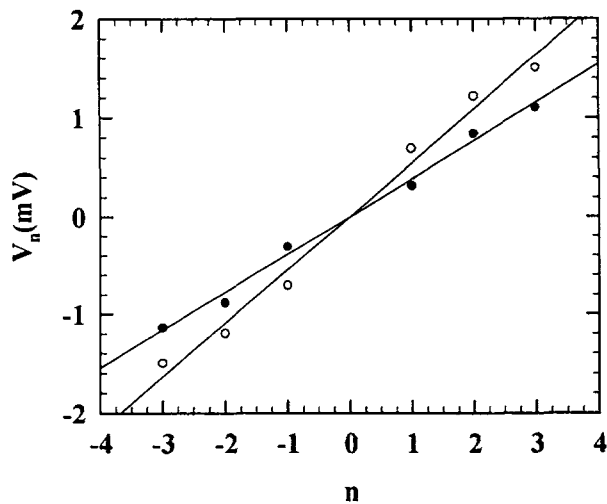


Fig. 6. Dependence of the voltage positions V_n as a function of the mode number n before (●) and after illumination (○).

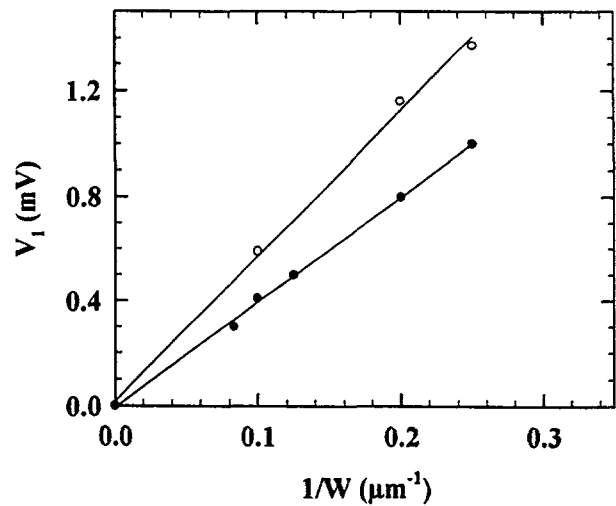


Fig. 7. Voltage position V_1 as a function of the inverse of the length W of the GBJJ before (●) and after illumination (○).

ACKNOWLEDGMENT

This work is supported by US-NSF and CNRS.

REFERENCES

1. A. Gilabert, A. Hoffmann, J. Elly, M. G. Medici, P. Seidel, F. Schmidl, and I. K. Schuller, *J. Low Temp. Phys.* **106**, 255 (1997); A. Hoffmann, I. K. Schuller, A. Gilabert, M. G. Medici, F. Schmidl, and P. Seidel, *Appl. Phys. Lett.* **18**, 2461 (1997).
2. V. I. Kudinov, A. I. Kirilyuk, N. M. Kreines, R. Laiho, and E. Lähderanta, *Phys. Lett. A* **151**, 358 (1990).
3. G. Nieva, E. Osquiguil, I. K. Schuller, and Y. Bruynseraede, *Appl. Phys. Lett.* **60**, 2159 (1992).
4. V. I. Kudinov, I. L. Chaplygin, A. I. Kirilyuk, N. M. Kreines, R. Laiho, E. Lähderanta, and C. Ayache, *Phys. Rev. B* **47**, 9017 (1993).

5. M. Maenhoudt Ph.D. Thesis, Katholieke Universiteit Leuven, Belgium (1995); J. Hasen, Ph.D. Thesis, University of California-San Diego, La Jolla (1995).
6. G. Nieva, E. Osquiguil, J. Guimpel, M. Maenhoudt, B. Wuyts, Y. Bruynseraede, M. B. Maple, and I. K. Schuller, *Phys. Rev. B* **49**, 3675 (1994).
7. For a short review see: A. Hoffmann, D. Reznik, and I. K. Schuller, *Adv. Mater.* **9**, 271 (1997).
8. J. Hasen, D. Lederman, V. Kudinov, M. Maenhoudt, and Y. Bruynseraede, *Phys. Rev. B* **51**, 1342 (1995).
9. P. Seidel, E. Heinz, F. Schmidl, K. Zach, H. J. Kohler, H. Schneidewind, J. Borck, L. Dorrer, S. Linzen, T. Kohler, W. Michalke, M. Manzel, E. Steinbeiss, H. Bruchlos, E. B. Kley, and H. J. Fuchs, *IEEE Trans. Appl. Supercond.* **3**, 2353 (1993).
10. M. G. Medici, J. Elly, A. Gilabert, F. Schmidl, T. Schmauder, E. Heinz, and P. Seidel, in *Applied Superconductivity 1995, Proceedings of EUCAS 1995, Edinburgh, United Kingdom, 3-6 July 1995, the Second European Conference on Applied Superconductivity*, D. Dew-Hughes, ed. (IOP, Bristol, United Kingdom, 1995), p. 1331.
11. D. Winkler, Y. M. Zhang, P. A. Nilson, E. A. Stepanov, and T. Claeson, *Phys. Rev. Lett.* **72**, 1260 (1995).
12. E. J. Tarte, F. Baudenbacher, J. Santiso, R. E. Somekh, G. A. Wagner, and J. E. Evetts, in *Applied Superconductivity 1995, Proceedings of EUCAS 1995, Edinburgh, United Kingdom, 3-6 July 1995, the Second European Conference on Applied Superconductivity*, D. Dew-Hughes, ed. (IOP, Bristol, United Kingdom, 1995), p. 1291.
13. A. Barone and G. Paterno, *Physics and Application of the Josephson Effect*, Wiley, New York (1982).
14. J. Elly, A. Gilabert, M. G. Medici, F. Schmidl, P. Seidel, A. Hoffmann, and I. K. Schuller, to be published in *Phys. Rev. B*, October 1997.